ISBN: 978-3-95450-132-8 doi:10.18429/JACoW-IPAC2014-THPME053

COST RATIONALES FOR AN SRF PROTON LINAC

F. Marhauser, Muons, Inc., Batavia, 60510 IL, USA

Abstract

Rationales to assess and minimize costs for a Superconducting Radio Frequency (SRF) proton linac are outlined. Operating frequency, velocity profile and temperature are regarded as variables when applicable. Hardware plus labor costs for cavities and cryomodules as well as expenditures for facility infrastructures including cryogenic systems, conventional facilities, and relevant subsystems are estimated. The focus is on the assessment of a 10 MW, 1 GeV Continuous Wave (CW) linac for an Accelerator Driven Subcritical Reactor (ADSR) [1].

INTRODUCTION

Expenditures for large-scale accelerator facilities typically range from a few hundred M$ to a few B$. Apart from capital expenses, one needs to account for operational costs accumulating over the years. The choice of operating frequency (f), temperature (T) and effective accelerating field (E_{acc}) not only affects the machines' footprint, but also the required capacity of the cryogenic plant. In parallel, one has to consider operational demands and limitations. A cost optimization is done for a proton CW linac using elliptical SRF cavities ('main' linac, 0.1-1 GeV), which covers the largest portion of the facility. Adequate low velocity CW structures ('front-end' systems) have not been scrutinized yet, though a cost estimate is included based on expenditures for the Spallation Neutron Source (SNS). Estimates are provided in 2013 year US $ throughout.

CAVITIES AND CRYOMODULES

One aim was to evaluate cavity and cryomodule (CM) costs without the specific knowledge of cavity geometries. The material costs of SRF cavities made from bulk Nb have been evaluated due to the required mass that scales with f and the velocity profile (β_g). Assuming a typical length of $1.5\cdot\beta_g\cdot c_0/(2f)$ for beam tubes (each side) and using a generic diameter $Ø(m) = 248.2/f(MHz)^{1.13}$, which is a fit function for known cavity geometries, yields the Nb costs for a bare cavity (f in GHz):

$$C_{cav} = N_c \cdot Nb_c(US\$/kg)\cdot 3.68\cdot t_w\cdot\beta_g^2\cdot f^{-2} + Nb_t(US\$/kg)\cdot 3.01\cdot t_w\cdot\beta_g\cdot f^{-2.13} \quad [\text{in US\$}]. \tag{1}$$

N_c denotes the number of cells and t_w (in mm) the wall thickness. The Nb price can be adjusted in both terms (also t_w) since one may use cheaper (low RRR) material for the tubes (index t) than for the cells (index c). Note that cavity prices from industrial vendors can be a few factors higher than the material costs. This still might not account for most of the auxiliary hardware. In fact, large expenses arise from the fundamental RF couplers. Costs of components may also scale with f. Using eq.(1) and estimating costs for an input coupler (SNS-type), tuner, two coaxial HOM couplers and a Helium vessel resulted in the numbers listed in Table 1 for 805 MHz proton cavities optimized for three different β_g-values.

Table 1: Cavity Parameter and Costs (t_w = 4mm) with and w/o Auxiliary Components (cf. text)

f (MHz)	β_g	N_c	L_{cav} (m)	cavity Nb costs/ plus components (k$)
805	0.47	6	0.79	26 / 113
805	0.61	6	1.07	44 / 138
805	0.81	6	1.29	77 / 182

L_{cav} is the sum of the active cavity length ($L_{act} = N_c\cdot\beta_g/2\cdot c_0/f$) and beam tubes. The rather broad velocity acceptance allows using only three β_g-sections from 0.1-1 GeV. Multiplying cavity expenses by the number of cavities per CM (N_{cav}) covers the majority of the cavity string hardware costs. Remaining string items plus CM hardware expenses have been estimated utilizing the CM work breakdown structure (WBS) of SNS (f = 805 MHz). Note that the CEBAF upgrade CM (f = 1.5 GHz) is based on the SNS concept, i.e. both are cryogenically segmented designs. These have the advantage of allowing the installation/exchange/repair of CMs individually, while adjacent CMs are kept cold. Focussing quadrupole magnets can be placed in the warm sections between CMs. Each CM consists of the outer insulating vacuum vessel housing a space frame, thermal and magnetic shielding, He pipes, and instrumentation, and He supply/return end cans. Down to a certain f (e.g. ~650 MHz for SNS CMs) one can install cavities within the same space frame/vessel [2]. Thus to first order, one can assume that the CM hardware costs mainly scale as a function of the CM length (L_{CM}), though the cavity string may still expand radially. This yields:

$$C_{CM} = 0.161\cdot L_{CM}(f,\beta_g) \quad [\text{in US M\$}]. \tag{2}$$

L_{CM} (in m, valve to valve) has to be kept within a practical limit. An extra $0.102\cdot N_{cav}+0.723$ (in m) is added beyond ($N_{cav}\cdot L_{cav}$) to account for overall beam line space requirements based on SNS (CEBAF CMs are packaged denser to save real estate). The WBS reveals that labor costs are about 30% of the hardware expenditures. E.g., combining eq.(1)-(2) (and adding cavity hardware) results in 2.4 M$ for a $\beta_g = 0.81$ SNS and 3.4 M$ for a $\beta_g = 1$ CEBAF CM, respectively. This is in good agreement with real expenses based on average costs. It also respects the (converging) learning curve of a series production.

FUNDAMENTAL RF LOSSES

In CW-mode, the fundamental (dynamic) RF losses (P_{RF}) in a cavity at cryogenic temperature are about an order of magnitude higher compared to pulsed machines

ISBN: 978-3-95450-132-8 doi:10.18429/JACoW-IPAC2014-THPME053

(few % duty factor). This demands sufficient He refrigeration capacity. Since P_{RF} in a cavity is given by

$$P_{RF} = \frac{E_{acc}^2 \cdot L_{act}^2}{R/Q \cdot G} \cdot R_s, \quad (3)$$

it is beneficial to increase the product R/Q·G by proper cell shape design. Reducing the cell aperture reduces the surface magnetic flux density (B_{peak}) at a given E_{acc} and provides a larger margin to quench limits. However, trade-offs with the aperture affects beam dynamics and mechanical stability (microphonics) of the cavities. The latter determines the power overhead for stable control, which adds expenses. The shunt impedance per cell $(R/Q)_c$ and the geometrical factor (G) have been generically evaluated from known designs ($0.4 \le \beta_g \le 1$):

$$\begin{aligned} (R/Q)_c &= -37.0(\pm 11.1)\,\Omega + 147.2(\pm 12.9)\,\Omega \cdot \beta_g \\ G &= 30.3(\pm 9.8)\,\Omega + 241.6(\pm 21.1)\,\Omega \cdot \beta_g . \end{aligned} \quad (4)$$

E_{acc} has to be chosen to reach the energy goal within a given footprint, while regarding $P_{RF} \sim E^2_{acc}$. The input power demands are driven by beam loading ($\sim I_{avg} \cdot E_{acc} \cdot L_{act}$). A medium field Q-slope or high field Q-drop, even in absence of field emission, can be detrimental since P_{RF} is proportional to the surface resistance ($R_s = G/Q_0$). Recent developments to eliminate the medium field Q-slope are encouraging [3]. However, the early onset of field emission still imposes prevalent operational limitations in existing facilities. The choice of E_{acc} is thus critical for the operational reliability and of particular importance for a proton driver of an ADSR. Without determining E_{acc} yet, one can define $P^*(\beta_g, f, T) = P_{RF}/(E_{acc}^2 \cdot L_{act})$, which normalizes the dynamical losses per unit of accelerating length. Thus, P* is a reasonable parameter for optimization studies depending on the machines' footprint. Substituting R_s with the sum of the BCS ($R_{BCS} = f^2 \cdot A/T \cdot e^{-\Delta/(k \cdot T)}$, $T < 0.5 \cdot T_c$, A is material parameter) and residual surface resistance (R_{res}) results in:

$$P^*(\beta_g, f, T) = \frac{L_c(\beta_g, f) \cdot \left(R_{BCS}(f,T) + R_{res}(f)\right)}{R/Q(\beta_g) \cdot G(\beta_g)}. \quad (5)$$

L_c denotes the cell length ($= \beta_g \cdot c_0/2f$). One does not need to define N_c yet. Note that R_{res} is a function of f too. R_{res} has been assessed based on experimental tests carried out at JLab spanning several years, which comprise 83 SNS, 24 ILC (1.3 GHz) and 83 CEBAF (refurbished) high purity, fine grain cavities [4]. Findings imply:

$$R_{res}(f) = a + b \cdot f^2. \quad (6)$$

86 CEBAF upgrade cavities have been added to yield a = 5.16 (±0.98) nΩ and b = 1.97 (±0.54) nΩ/GHz^2. Combining eq.(5) and (6) and evaluating the minimum of P^* with respect to f provides the optimum frequency (f_{opt}) given by eq.(7). If R_{res} would be constant, the term (b·T) would vanish and $R_{BCS}(f_{opt}) = R_{res}(f_{opt})$. Due to this term however, f_{opt} will be smaller accordingly and $R_{BCS}(f_{opt}) \neq R_{res}(f_{opt})$, whereas $R_s(f_{opt}) = 2a$ and hence independent of T.

$$f_{opt} = \sqrt{\frac{a \cdot T}{A \cdot e^{-\frac{\Delta}{k_B \cdot T_C} \cdot \frac{T_c}{T}} + b \cdot T}}. \quad (7)$$

As an example, Fig. 1 plots $P^*(f)$ for three β_g-values at T = 2 K and a trend, when T is reduced (2-1.6 K) for $\beta = 1$. To compute and scale $R_{BCS}(f, T)$, reference data for fine grain Nb cavities (f = 1.3 GHz, T = 2 K) have been utilized (after BCP/EP and a low-T bake). E.g., the optimum frequency at 2 K is 0.93 GHz. A lower T shifts f_{opt} upwards and decreases P* as expected. However, since there is a price to pay to cool down the Helium, one needs to account for refrigeration costs simultaneously.

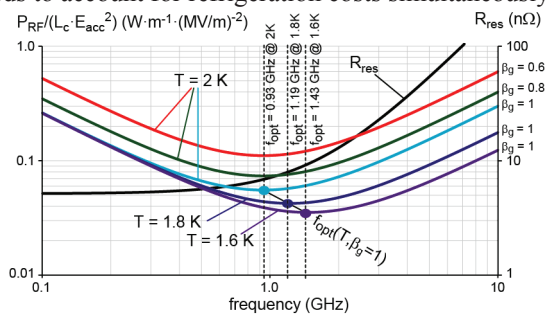

Figure 1: Normalized dynamical RF losses (cf. text).

HELIUM REFRIGERATION

For the capital cost assessment of the main Helium cold box (4.5 K) the equivalent refrigeration capacity at 4.5 K (R) has been calculated. It primarily depends on the non-isothermal refrigeration load (Q_{ref}) absorbed by the system between 4.5 K and a He recovery temperature (T_R) determined by the cold compressor box (CCB). Ref. [5]-[6] provide scaling laws for 4.5 K refrigerators as a function of capacity. The combined data yield (in M$):

$$C1 = 3.0 \cdot R^{0.63} [\text{R in kW @ 4.5K}]. \quad (8)$$

The capital costs of the CCB are assessed separately adapting the LHC cost models [7] as given by C2 and C3 (in M$, factor ~1 for CHF/USD conversion and inflation):

$$C2 = 0.5 \cdot (25.7 \cdot (Q_{op}/P_R)^{0.6} - 0.45)$$

$$C3 = \sum_{j=1}^{N} \left[0.62 \cdot \left(\dot{m}_0 \cdot \sqrt{T_{0,j}} / P_{0,j} \right)^{0.33} + 0.71 \cdot W_{0,j}^{0.33} \right]. \quad (9)$$

C2 holds for an integral cold compression (CC) cycle (no warm compressor here). Q_{op} is the load (in kW) at He temperature. He recovery pressure from the CCB is at P_R (in kPa). C3 comprises the costs for each single CC stage based on the inlet parameters, namely the mass flow ($\dot{m}_0$ in kg/s), temperature ($T_{0,j}$ in K), pressure ($P_{0,j}$ in kPa), and compression power ($W_{0,j}$ in kW). To assess the equivalent load at 4.5 K arising from the He cavity bath temperature, the ratio $r = Q_{ref}/Q_{op}$ has been evaluated for several CCB

ISBN: 978-3-95450-132-8 doi:10.18429/JACoW-IPAC2014-THPME053

models varying T within 1.6-2.1 K. Reasonable constraints have been obeyed (cf. [7]). The number of CCs depends on the assumption of individual pressure ratios (PR). Assuming five CCs for all models, while never exceeding PR = 3 and keeping P_R and T_R fixed throughout, yields eq.(10) (fit, 1.6 K ≤ T ≤ 2.1 K, R^2~1).

$$r\,(W@4.5K/W@T) = 0.24 \cdot T^2 - 1.67 \cdot T + 5.88 \qquad (10)$$

Applying eq.(10), one can now sum up $P^*(\beta_g, f, T)$ over all CMs to evaluate the equivalent losses at 4.5 K in order to estimate the costs for the refrigerator. One also needs to assess the dynamic losses arising from other components (e.g. input and HOM couplers, bellows). Moreover, all static losses dissipated via conduction and radiation as well as intercepted at thermal shield(s) within the CM need to be assessed and converted to 4.5 K. These losses have been itemized and partially parameterized in terms of the dependence on L_{CM} (not detailed here). The dynamic and static losses have been summed up (incl. liquefaction demands, losses in transfer lines, beam losses (1W/m)) for each β_g-section of the linac. Figure 2 visualizes the equivalent load at 4.5 K in dependence on f and T.

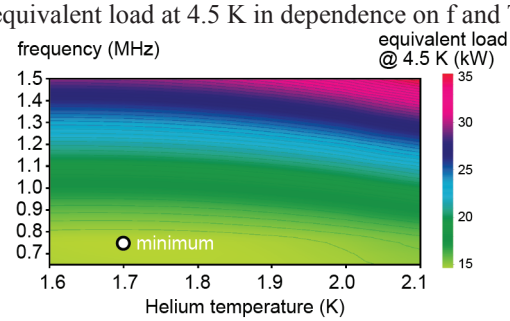

Figure 2: Equivalent dynamic and static losses at 4.5 K for the proton linac covering three β_g-sections (cf. text).

Herein values for R/Q and G are computed for realistic cavity designs. Fig. 2 also reveals at which f and T the technical limit for a single refrigeration plant (~18 kW @ 4.5 K) is exceeded. Frequencies below ~1 GHz are thus favoured at all temperatures. The effective voltage (on crest) has been kept constant in each β_g-section by defining reference values for E_{acc} at 805 MHz, which were 11.3, 11.9, and 13.2 MV/m with ascending β_g. Consequently, 1 GeV has been achieved with the same number of CMs throughout, which are 9 at $\beta_g = 0.47$, 11 at $\beta_g = 0.61$, and 13 at $\beta_g = 0.81$, respectively. Note that the optimum f is now smaller than implied by Fig. 1. The minimum cryogenic losses occur at $f_{opt} \approx 750$ MHz and T ≈ 1.7 K, respectively, though it is a shallow minimum. For this reason, the operating temperature has no dramatic impact on costs. It rather can be chosen to reduce the complexity of the CCB (e.g. number of CC stages and combined PR). The tunnel length in Fig. 2 and associated costs may vary. A similar calculation has been done by changing the number of CMs and keeping E_{acc} (values mentioned above) and tunnel length constant throughout. However, this always increased the losses at 4.5 K in comparison. Based on the findings, an RF frequency of 805 MHz for the main linac - close to the optimum - is deemed a good choice since this frequency (and hardware) is already employed at SNS. The aforementioned E_{acc}-values actually minimize the equivalent losses at 4.5 K, which amount to 15.4 kW when operating at T = 2 K. It includes contingencies to also keep in mind He demands for SRF front-end systems. The E_{acc}-levels guarantee $B_{peak} < 80$ mT in each cavity type, which is below the typical onset of a high-field Q-drop and also reasonably low to mitigate field emission. Moreover, input coupler technology (e.g. SNS-type coupler) is capable to provide the required power levels (plus overhead) at 10 mA average current.

OVERALL COSTS AND CONCLUSION

With present assumptions, the main linac is ~206 m long to obtain 1 GeV (starting at 100 MeV). To estimate the overall costs of the proton driver, the WBS of the SNS linac facility (1.4 B$ in 2008) has been scrutinized. Obsolete/extraneous expenses have been omitted (e.g. accumulator ring and systems) as well as those that can be budgeted for on the reactor side instead (e.g. target, non-accelerator instrumentation systems). Since the SNS construction period covered one decade, appropriate cost inflation has been done. Itemized expenses include R&D and project support (each ~$58 M$), front-end systems (~28.5 M$), linac systems (~412 M$), conventional facilities (~287 M$), integrated control systems (~61 M$), and pre-operations (~79 M$). This sums up to ~982 M$ in total. The linac systems include the reassessment of the CM costs (~34 M$) and the cryogenic system (~43 M$) according to the scaling laws described above. For the latter, eq.(9)-(10) sum up to ~21 M$, yet the costs for the central He building itself, He transfer and distribution, ancillary equipment lines plus labor costs for design and commissioning are adding slightly more than 50%. With RF input power overhead (25%), klystron efficiency (50%), He plant efficiency and demands for the low conductivity water system (assuming 35% of RF power) the AC wall plug power for a 10 MW machine is 37.4 MW (27% efficiency). This will determine the operational costs, which is a cost driver depending on yearly operating hours and local electricity prices. As a benefit of an ADSR, a small portion of the generated power can be fed back again to power the proton driver.

ACKNOWLEDGMENT

The author likes to thank D. Arenius, G. Ciovati, A. McEwan, T. Powers, and R.A. Rimmer for fruitful discussions relevant to this work.

REFERENCES

[1] R.P. Johnson et al., Proc. IPAC 2013, THPWA047.
[2] R.A. Rimmer, ADS workshop, VTech, 2010.
[3] A. Grassellino, Proc. SRF2013, TUIOA03.
[4] G. Ciovati et al., IEEE Trans. Appl. Superconduct., Vol. 21, No. 3, June 2011.
[5] M.A. Green, Technical Note LBNL-63506, 2008.
[6] S. Claudet et al., LHC Project Report 317, 1999.
[7] S. Claudet et al., LHC Project Report 391, 2000.